Characterizing Strain Induced by Environmental Loads in Jointed Plain Concrete Pavements

Immediately After Paving and Throughout First 10 Months

Steven A. Wells, Brian M. Phillips, and Julie M. Vandenbossche

The focus of this study is to provide a detailed analysis of the strain that develops as a result of environmental loads. The study characterizes slab response immediately after construction (first 72 h after paving) and also addresses seasonal effects over the first 10 months following construction. A heavily instrumented test section was constructed on SR-22 in Murrysville, Pennsylvania, to help characterize slab response to environmental loads better. Static strain and climatic data collected through the first 10 months after construction (August 2004 through June 2005) were analyzed to interpret pavement response to environmental loads as a function of location with respect to joint proximity, depth within the slab, and level of restraint applied to the slab. Many things were also learned about the strain that develops in the slab over the first 10 months after construction. The average strain in the fall was around –450 μstrain, whereas the average strain in the winter was –600 μstrain. The ambient temperatures increased during the spring and summer; this resulted in a decrease in the average strain to –250 μstrain. Thermal strain was found to be twice as high as the drying shrinkage the first winter after construction. A substantial amount of drying shrinkage occurred within the first 50 days after construction. Variations in drying shrinkage occur not only through the depth of the slab but also across the surface of the slab.

The trend to move toward a more mechanistic approach in jointed plain concrete pavement (JPCP) design has emphasized the need to more accurately characterize pavement response to environmental and vehicle loads (*1*). Finite element analysis has been the commonly used tool for calculating pavement stress. It is important to validate these theoretical models with field data since the restraint in thermal- or moisture-related deformation caused by the self-weight of the slab and the friction between the bottom of the slab and underlying layers and tie and dowel bars and the shoulder is rather complex and difficult to model. Since stress cannot be measured directly, strains are typically measured in the field. Stress develops when the slab is not allowed to expand or contract freely with changes in temperature or moisture content. Stress generated within the slab can be quantified by characterizing the reduction in strain that occurs with changes in moisture content and temperature as a result of the restraint conditions just described. The focus of this study is to provide a detailed analysis of the strain that develops as a result of environmental loads.

University of Pittsburgh, Pittsburgh, PA 15261.

Transportation Research Record: Journal of the Transportation Research Board, No. 1947, Transportation Research Board of the National Academies, Washington, D.C., 2006, pp. 36–48.

This study characterizes slab response immediately after construction (first 72 h after paving) and also addresses seasonal effects over the first 10 months following construction.

DESCRIPTION OF INSTRUMENTED TEST SECTION

A heavily instrumented test section was constructed on SR-22 in Murrysville, Pennsylvania, to help better characterize slab response to environmental loads. The pavement consists of a 12-in. JPCP constructed on top of a 4-in. asphalt-stabilized base and 5 in. of densely graded subbase. The pavement is a four-lane divided highway, and each lane was paved independently. The instrumentation was placed in the outside westbound lane. The inside westbound lane was paved a month before the outside lane. The test section was paved on August 1, 2004, at approximately 7:00 a.m. A curb and gutter were tied onto the westbound lanes at the end of October. The pavement contained 1.5-in. dowels along the transverse joints and No. 5 tie bars spaced 3 ft on center along the centerline joint. The dowel and tie bars were left out of six slabs so the effect of the restraint they impose on the slab could be quantified. The transverse joint spacing was 15 ft.

Ambient conditions were measured in the field with an on-site weather station, and thermal gradients were captured using thermocouples embedded throughout the depth of the pavement. The instrumented pavement also contained static and dynamic strain gauges and pressure plates (*2*). Each sensor location was replicated three times in three consecutive slabs. The focus of this study was on the static strain gauge and climatic data collected at the test section. These data include three restrained slabs and three unrestrained slabs fully instrumented with static strain gauges. An automated data collection system was used to collect and store data every 15 min. The data logger was automatically downloaded every 24 h via modem and dumped in a database on a computer housed at the University of Pittsburgh. The static strain gauges are Geokon 4200 vibrating wire strain gauges.

The data collected through the first 10 months after construction (August 2004 through June 2005) were analyzed to interpret pavement response as a function of location with respect to joint proximity, depth within the slab, and level of restraint applied to the slab. Strain data at the top (1 in. from the surface) and bottom (1 in. from the bottom) of the slab and at several locations within the slab for both restrained and unrestrained slabs were analyzed. The gauge locations are described below and shown in Figure 1;

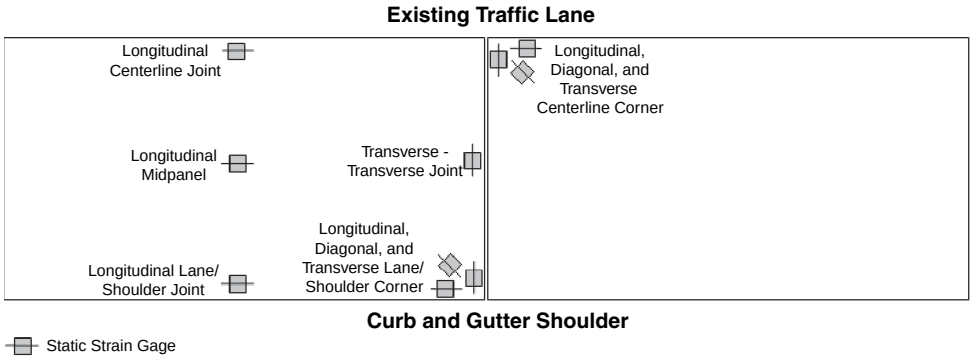

FIGURE 1 Summary of vibrating wire strain gauge locations within panel.

- Adjacent to the lane–shoulder joint at midpanel oriented in the longitudinal direction;
- At midpanel oriented in the longitudinal direction;
- Adjacent to the centerline joint at midpanel oriented in the longitudinal direction;
- Adjacent to the transverse joint in the center of the lane oriented in the transverse direction;
- Adjacent to the lane–shoulder (L-S) joint corner oriented in the longitudinal, transverse, and diagonal directions; and
- Adjacent to the centerline joint corner oriented in the longitudinal, transverse, and diagonal directions.

Creep and fluctuations in moisture and temperature in the concrete will affect the measured strains (*3*–*5*). Equation 1 accounts for the thermal, moisture, and creep contributions toward concrete strain, also referred to as actual strain:

$$\mu_{m,c,t} = (R_1 - R_0)B + (T_1 - T_0)(C_1) \quad (1)$$

where

$\mu_{m,c,t}$ = strain influenced by creep, moisture, and temperature changes,
R_0 = raw strain at time$_0$ (initial concrete set),
R_1 = raw strain at time$_1$,
T_0 = temperature at time$_0$,
T_1 = temperature at time$_1$,
C_1 = thermal coefficient of expansion of steel in strain gauge = 6.78 μstrain/°F, and
B = batch calibration factor (provided by manufacturer).

The estimated time of set of 10 h was based on static strain. Figure 2 shows strain versus change in temperature. The set time was defined as the time that strain began to develop with changes in temperature. The set time of the concrete was approximately 10 h after construction.

STRAIN RESPONSE 72 H AFTER PAVING

Strain gauges are used to measure deformation caused by moisture and temperature changes. Stress will not develop if the slab is free to deform when changes in temperature and moisture occur. It is when this deformation is restrained that stresses develop. The deformation is restrained primarily by the friction between the bottom of the slab and the base, the dowel and tie bars, and the weight of the slab itself (*3*, *6*). An analysis is provided next of the strain measured during the first 72 h after paving, a time period when the concrete gains a large portion of its strength (and stiffness). Strain will be investigated with respect to depth, location, and restraint within the JPCP as well as strain continuity across joints.

Depth, Location, and Restraint

Figure 3 compares strain measured at four different locations within unrestrained slabs during the first 72 h after construction. As shown, readings were taken at two different depths, 1 in. from the surface and 1 in. from the bottom of the pavement. Both graphs show that the largest strain is measured along the transverse joint because with the absence of a curb and gutter, there is no restriction on movement from the outside portion of the slab. The longitudinal strain along the centerline exhibits the lowest strain in both cases since movement is restrained by the presence of the inside lane. The magnitude of the strain decreases with increasing slab depth, which indicates that the bond between the base and the bottom of the slab is sufficient to restrain slab deformation. Also, the temperature fluctuations at the bottom of the slab are less than those at the top of the slab.

Similar comparisons were performed for the restrained slabs (Figure 4). The largest strain was measured along the transverse joint in the transverse direction, and the smallest strain was found along the centerline joint in the longitudinal direction. Also, as was

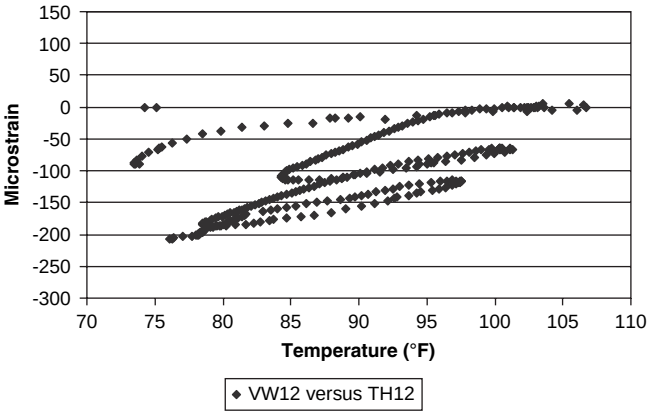

FIGURE 2 Strain versus temperature at bottom of slab at midpanel for first 72 h after paving.

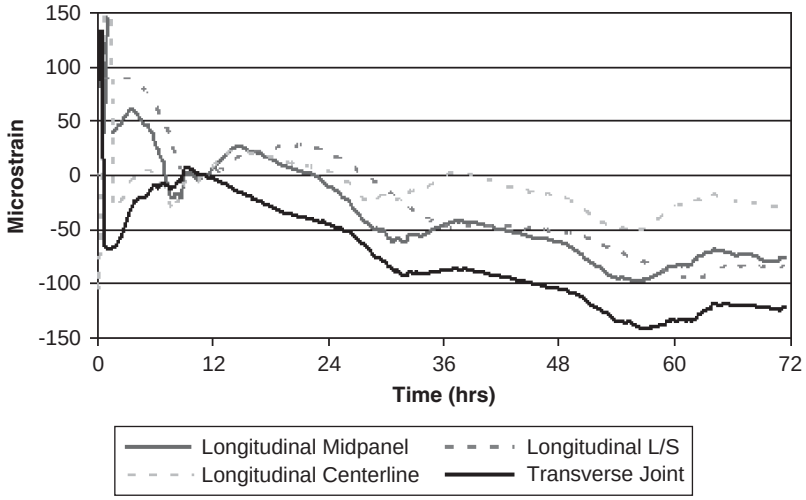

(a)

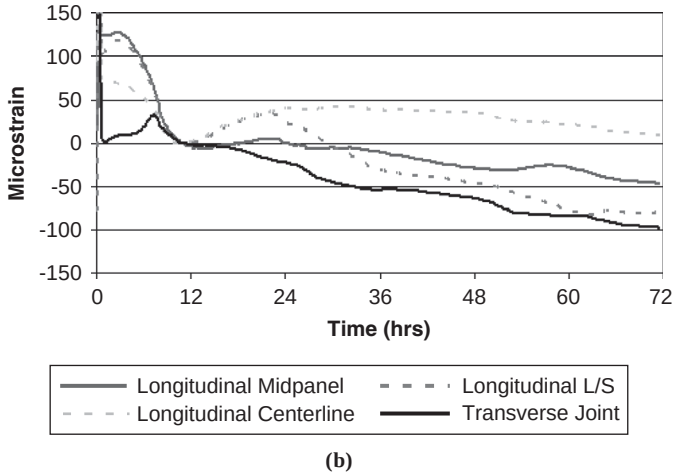

(b)

FIGURE 3 Strain measured at (*a*) top and (*b*) bottom of unrestrained slab.

seen for the unrestrained slabs, strains measured at the bottom of the slab were lower than the strains measured at the top of the slab.

In comparing the strains measured in the restrained slabs with those in the unrestrained slabs, the spatial variation in the magnitude of measured strain was greater for the unrestrained slab compared with the restrained slab. The strains appear more uniform across the slab for the restrained slabs. In general, the strains for the restrained slab appear to be lower than those for the unrestrained slab. This finding can be attributed to the fact that the slab is tied to the previously constructed inside lane. The stiffness of the concrete in the inside lane would be higher than that of the concrete in the outside lane since this analysis is looking at strains measured within the first 72 h after paving of the inside lane.

Uniformity of Strain on Opposing Sides of Transverse Joint

To evaluate the uniformity of the strain on opposing sides of a transverse joint, strains measured in the corner adjacent to the lane–shoulder joint on both the approach and leave sides of the transverse joint were compared. This comparison is made to determine how uniform the strain is throughout the pavement section. Strains measured in the longitudinal, diagonal, and transverse directions are shown in Figure 5. Little difference is seen in the magnitude of the strain between unrestrained and restrained slabs along the transverse joint. This finding most likely is because the curb and gutter have not yet been constructed, so the restraint conditions along the lane–shoulder joint are similar. Both graphs show good correlation between strains measured on opposite sides of the joint but in the same direction. There is a slight discrepancy between the diagonal strains in the unrestrained slabs. Since the longitudinal and transverse strains are similar, this discrepancy is most likely the result of the orientation of the diagonal sensor on the approach side, which was installed in a slightly more transverse direction and thus produced readings similar to those of the transverse sensors.

Centerline and Lane–Shoulder Joint

Figure 6 shows the strains measured in the corner along the lane–shoulder joint and in the corner along the centerline joint. These strains were measured adjacent to the same transverse joint to eliminate possible discrepancies that could be attributed to differences

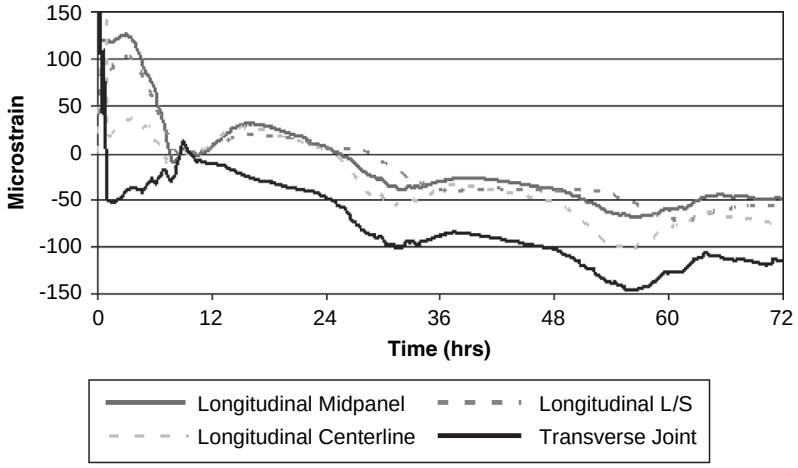

(a)

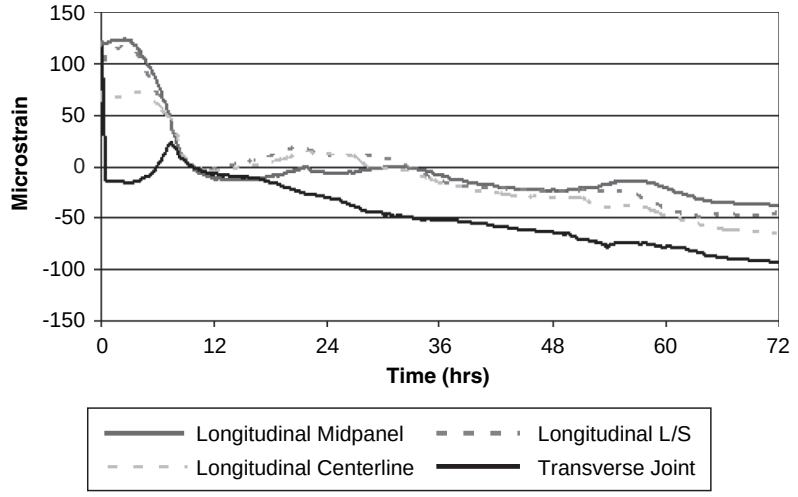

(b)

FIGURE 4 Strain measured at (*a*) top and (*b*) bottom of restrained slab.

in joint width. For the unrestrained slabs, Figure 6*a* shows that the strain in all directions is similar on the lane–shoulder side. Restraint associated with the boundary conditions was limited since no curb and gutter are present and the crack at the joint was quite wide. At the centerline, the strain in the transverse direction is similar to that in the opposing corner near the lane–shoulder joint. However, in the longitudinal direction the strain is lower because of the restraint imposed by the previously constructed adjacent lane. The restraint in the longitudinal direction also affected the strain measured along the diagonal. The decrease in strain between that measured in the traverse direction compared with the longitudinal and diagonal along the centerline joint was about 50 μstrain. This measurement correlates with a stress of 180 psi. Strains measured in the restrained slabs (Figure 6*b*) exhibited a similar response.

Effect of Crack Width on Strain

When the joints cracked after sawing, the relative width of the crack was recorded. The strains measured in the corner near joints with different crack widths were compared to evaluate the effect of joint width on the measured strains. Figure 7 compares strains measured in the corner near the centerline and adjacent to a transverse joint with a wide crack and a transverse joint with a narrow (tight) crack. The strains were similar regardless of crack width with the exception of strains measured along the diagonal. This finding is probably because the orientation in which the gauge was installed was not exactly 45 degrees from the direction of traffic.

SEASONAL STRAIN RESPONSE DURING FIRST 10 MONTHS AFTER PAVING

The graphed strain for the analysis of the variation in strain throughout the depth of JPCP slabs through seasonal temperature and moisture fluctuations includes strain induced by temperature, moisture, and creep calculated using Equation 1. As a pavement undergoes changes in thermal and moisture conditions, the strain response between the top and bottom of the slab can be quite different. Diurnal and seasonal factors such as nonuniform drying shrinkage throughout the depth of the slab, subgrade temperature and moisture, ambient conditions, and frictional restraint at the PCC–base interface can contribute to signif-

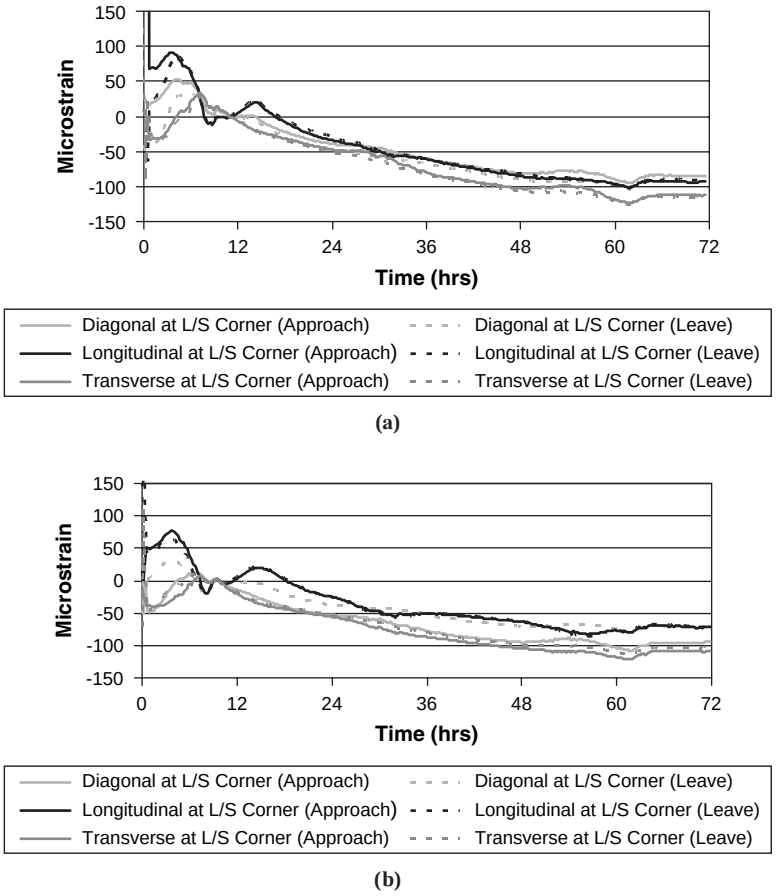

FIGURE 5 Strain measured in corner adjacent to lane–shoulder joint on both approach and leave sides of transverse joint.

icant differences in the strain, and hence stress, response between the top and bottom of JPCP slabs.

Seasonal Variation in Strain

Depth, Location, and Restraint

As shown in Figure 8*a*, the strain measured in October, shortly (2 months) after construction, is negative at the top and bottom of the slab. This finding can be explained by the fact that the temperature throughout the depth of slab at the time of setting is higher than the slab temperatures typically encountered during the month of October. As the overall ambient temperature decreases, the length of the slab decreases. Another interesting observation is that the strain at the top of the unrestrained slab is greater than that at the bottom. This phenomenon can be attributed to the higher degree of drying shrinkage that takes place at the surface compared with the bottom of the slab. The daily fluctuations in temperature throughout the depth of the slab can also be seen in Figure 8*a*.

As ambient temperatures drop in the winter, the measured strains become increasingly negative, as indicated in Figure 8*b*. The average strain in the fall was around −450 μstrain, whereas the average strain in the winter was −600 μstrain. The diurnal temperature swings also decrease in the winter because of prevailing seasonal temperature patterns and length of daylight hours. The resulting response is a decrease in diurnal strain fluctuations when strains measured in the fall (Figure 8*a*) are compared with those measured in the winter (Figure 8*b*). The drying shrinkage at the surface of the slab also appeared to be slightly higher in the winter than in the fall. Factors contributing to this shrinkage are the lower humidity and fewer precipitation events in the winter. In addition, a substantial amount of drying shrinkage will occur in the first 90 days after construction.

Strains measured in the summer (June) are shown in Figure 8*c*. Ambient temperatures increase during the spring and summer, which results in a decrease in the average strain from −600 μstrain in the winter to −250 μstrain in the spring and early summer. Figure 8*c* shows that the daily strain fluctuations are also much larger in the summer than in the winter (Figure 8*b*). The reason can be the fact that there are higher temperature fluctuations in the spring and summer. These temperature fluctuations are much larger on the surface than at the bottom of the slab, and this condition is reflected in the larger strain fluctuations measured on the surface of the slab.

This behavior was found to be quite similar for restrained slabs. Figure 9 shows the strain at the top and bottom of a restrained slab over the same time period during the winter.

Comparing Figures 8*b* and 9, it appears that restraint has a negligible influence on strain differentials between the top and bottom of the slab in the longitudinal direction. Although the overall strain is consistently less for the restrained slabs, the disparity between strains throughout the depth of the slab is comparable with that of an unrestrained slab.

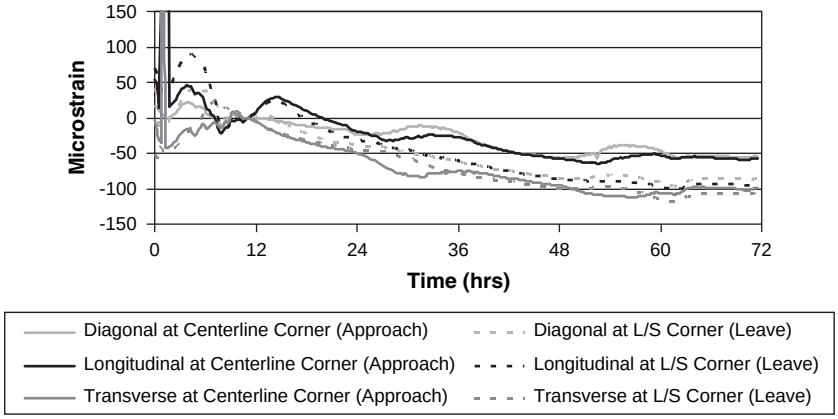

(a)

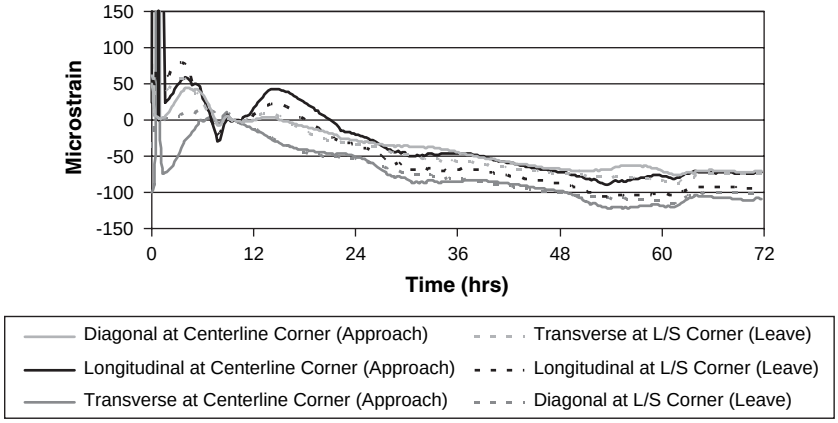

(b)

FIGURE 6 Strains measured in corner along lane–shoulder joint and in corner along centerline joint.

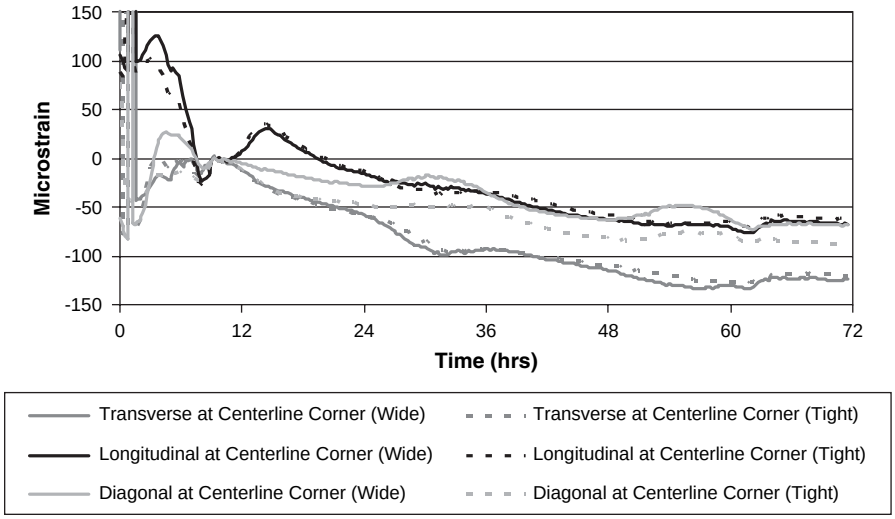

FIGURE 7 Strain at centerline of two different joints for unrestrained slab.

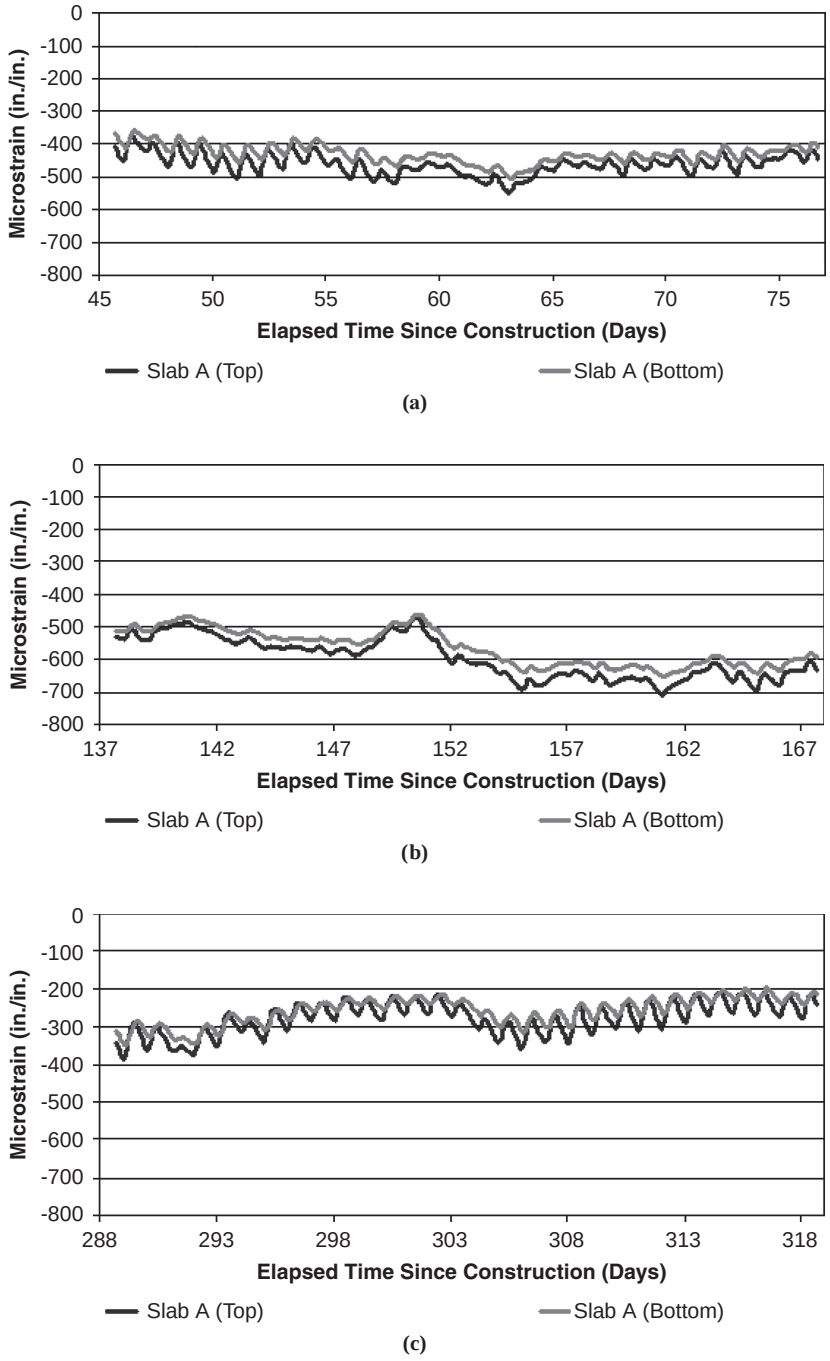

FIGURE 8 Static strain measured along lane–shoulder joint for unrestrained slab.

Position Within Slab and Level of Restraint

For the analysis of position within the slab and level of restraint, pavement temperatures measured in the field were plotted against the corresponding strains. The level of restraint was quantified through the thermal strain rate (TSR), defined by plotting strain versus temperature and then performing a linear regression analysis. The slope of this line is defined as the TSR, which is similar to the thermal coefficient; however, the thermal coefficient of expansion is a concrete material property, whereas the TSR represents the combined effect of the material properties and the structural characteristics of the pavement. Differences in the TSR provide an indication of the level of restraint present at each location. Strains measured in the spring (April) were chosen for this analysis. The range of temperatures experienced for a particular location within a slab is greatest in the spring. These large variations in temperature provide a greater range of data points over which to make a more accurate evaluation of the TSR.

Figure 10*a* shows the distribution of strain across the top of an unrestrained slab. As expected, the overall strain at the centerline joint is the smallest because of the restraint provided by the adjacent slab. The largest strain was measured adjacent to the lane–shoulder

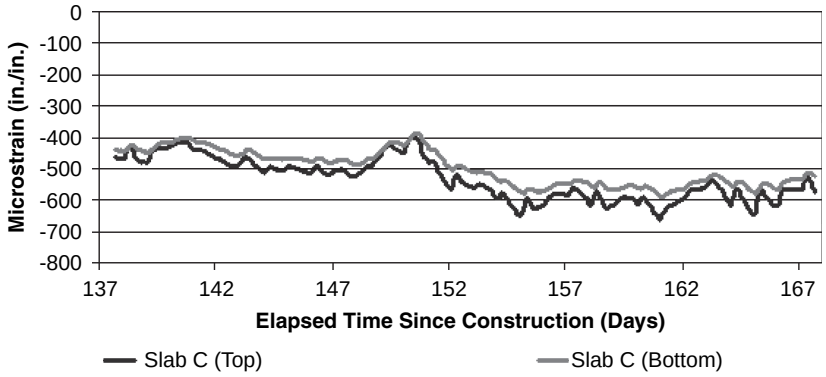

FIGURE 9 Static strain measured in winter along lane–shoulder joint for restrained slab.

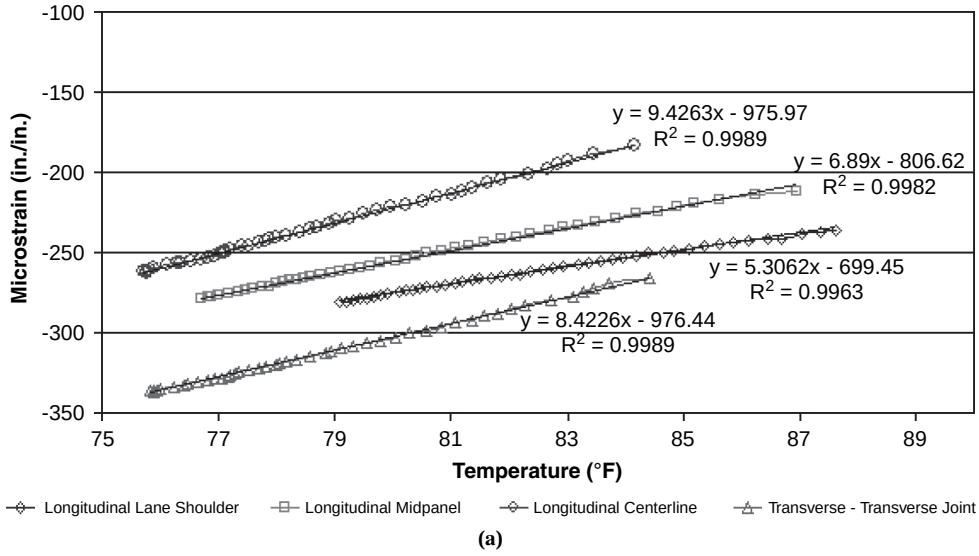

(a)

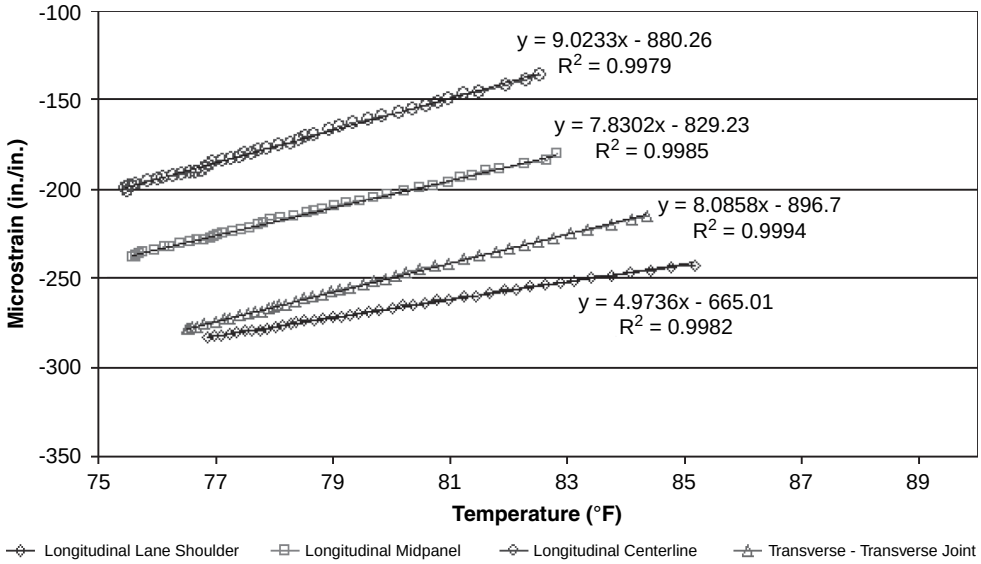

(b)

FIGURE 10 Temperature versus strain measured at top of (*a*) unrestrained slab and (*b*) restrained slab in spring.

joint in the longitudinal direction. The TSR at the lane centerline was the largest and that at the lane–shoulder joint was the smallest. Figure 10*b* shows the same trends for a restrained slab.

Figure 11 shows the distribution of strain at the bottom of the slab. It is evident that overall strains are less at the bottom of the slab than at the top for both restrained and unrestrained slabs. This finding is due to the frictional resistance provided by the base material and the higher moisture content at the bottom of the slab compared with the top of the slab.

Table 1 summarizes the TSR values obtained from Figures 10 and 11 The top of the table summarizes the difference in strain for each location at the top of the slab, and the bottom summarizes the difference in strain for each location at the bottom of the slab. From Table 1, it can be seen that the reduction in strain with changes in temperature at locations near the joints is approximately 0.34 to 0.41 μstrain/°F. This finding indicates that the dowel and tie bars do restrain thermal deformation in the slab. The opposite effect is apparent at midpanel, with a higher rate of strain with changes in temperature occurring at midpanel for the restrained slabs. Restraint creates a redistribution of strain concentrations in which strain is reduced at locations near the joints but is increased at locations further away from the joints.

It is evident that restraint has a greater effect on slab movement at the bottom of the slab than at the top. The design thickness of the slab was 12 in. but the as-built thicknesses were up to 14 in., so the tie and dowel bars were most likely located closer to the bottom of the slab than to the top. This location would produce a higher level of restraint near the bottom of the slab. (Strain comparisons were

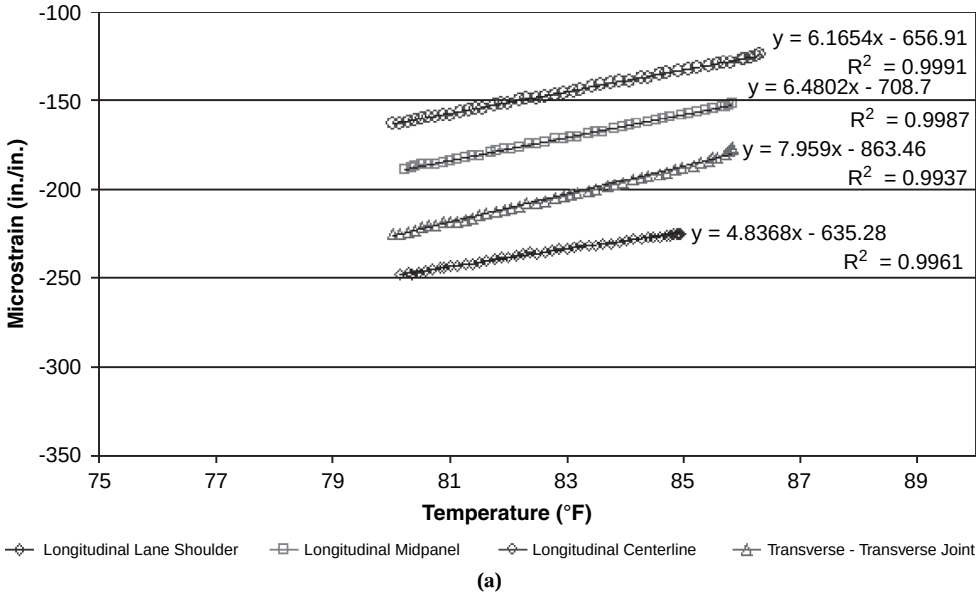

(a)

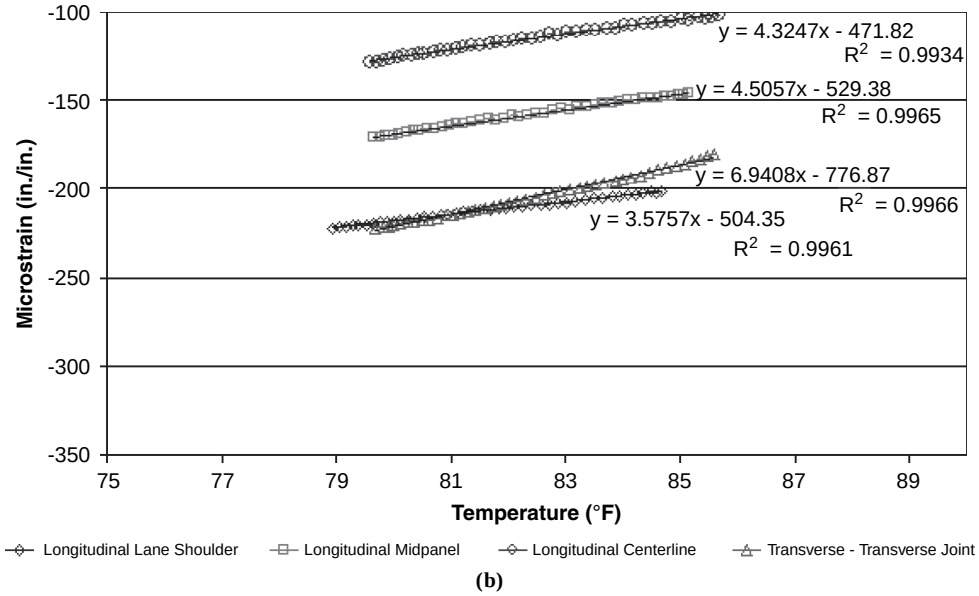

(b)

FIGURE 11 Temperature versus strain measured at bottom of (*a*) unrestrained slab and (*b*) restrained slab in spring.

TABLE 1 Thermal Strain Rates at Top and Bottom of Slab

Restraint Condition	Thermal Coefficient (in./in./ºF)			
	Longitudinal Lane/Shoulder	Longitudinal Midpanel	Longitudinal Centerline	Transverse Joint
Summary of restraint for top sensors				
Unrestrained	5.31E-06	6.89E-06	9.43E-06	8.43E-06
Restrained	4.97E-06	7.83E-06	9.02E-06	8.09E-06
Difference	3.40E-07	–9.40E-07	4.10E-07	3.40E-07
Summary of restraint for bottom sensors				
Unrestrained	4.84E-06	6.48E-06	6.17E-06	7.96E-06
Restrained	3.58E-06	4.51E-06	4.32E-06	6.94E-06
Difference	1.26E-06	1.97E-06	1.85E-06	1.02E-06

made only between locations with similar slab thicknesses.) At locations adjacent to the joints, the difference in restraint between restrained and unrestrained slabs is 3 to 4.5 times greater for bottom sensors than for top sensors. As with the top of the slab, the difference between restrained and unrestrained slabs at midpanel location is the greatest. Unlike the top, restraint reduces midpanel strains.

Table 2 is a summary of the combined effects of moisture-related shrinkage, creep, and restraint at the time of set and equivalent set temperature as established by the regression equations defined in Figures 10 and 11. The moisture-related shrinkage was estimated by determining the strain (y) when the temperature (x) is equal to the temperature at the time the concrete set. The equivalent set temperature was estimated by solving for temperature (x) when the strain (y) is equal to zero. These values are not representative of the concrete material properties but of the combined effect of the material properties and the structural characteristics of the pavement, similar to the relationship between the TSR and the thermal coefficient of expansion described earlier.

Columns 1 and 4 in Table 2 represent the moisture-related shrinkage at the time of set considering creep and the restraint of moisture- and temperature-related deformation. Similar degrees of drying occur in both slabs, but the dowel and tie bars restrain the shrinkage that occurs with equivalent reductions in moisture. The moisture-related shrinkage is substantially higher along the lane–shoulder edge because this edge did not have a tied shoulder at the time of paving and thus was exposed to ambient environmental conditions and the shrinkage was not restrained.

The equivalent set temperature determined by solving for x was similar to the actual set temperatures determined using the technique presented in Figure 2. The actual set temperatures tended to be lower at the bottom of the slab compared with the top since paving took place early in the morning when the asphalt base was quite cool. The slab in the adjacent lane was also quite cool, which resulted in lower actual set temperatures along the centerline joint compared with the set temperatures at midslab or along the lane–shoulder joint. The actual set temperature along the lane–shoulder joint was lower than that at midslab since it was exposed to the low ambient temperatures experienced at this time of day.

The equivalent set temperature represents the zero strain condition at the time of set when moisture- and temperature-related shrinkage, creep, and restraint are considered. The equivalent set temperature and actual set temperature are very similar. The exception is along the lane–shoulder joint, where the equivalent set temperatures are much higher than the actual set temperatures because the moisture-related shrinkage is significantly higher at this edge since the tied shoulder was not constructed until a couple of months after paving, as previously described.

TABLE 2 Combined Effects of Moisture-Related Shrinkage, Creep, and Restraint at Time of Set and Equivalent Set Temperature at Top and Bottom of Slab

		Unrestrained Slabs			Restrained Slabs		
		Moist., Creep, & Restraint (με)	Actual Set Temp. (°F)	Equiv. Set Temp. (°F)	Moist., Creep, & Restraint (με)	Actual Set Temp. (°F)	Equiv. Set Temp. (°F)
Top of slab	Centerline	–64	97	104	–22	95	98
	Midpanel	–75	106	117	–23	103	106
	L/S	–151	103	132	–174	99	134
	Transverse	–103	104	116	–66	103	111
	Average	–98	102	117	–71	100	112
Bottom of slab	Centerline	–70	95	107	–60	95	109
	Midpanel	–41	103	109	–66	103	117
	L/S	–155	99	131	–159	97	141
	Transverse	–42	103	108	–76	101	112
	Average	–77	100	114	–90	99	120

Effects of Drying Shrinkage and Creep

Moisture gradients have a profound effect on the shape of the slab (*7, 8*), effects of moisture-related shrinkage, and the restraint conditions in the slab. The effects of moisture-related shrinkage, creep, and restraint conditions at locations within the slab throughout the year are considered in this section. These components are isolated from temperature-induced strain in this analysis by using Equation 2:

$$\mu_{m,c} = (R_1 - R_0)B + (T_1 - T_0)(C_1 - C_2) \quad (2)$$

where $\mu_{m,c}$ is the strain influenced by creep and moisture changes, C_2 is the thermal coefficient of expansion of the concrete (5.71 μstrain/°F, measured in the laboratory), and the other terms are as defined for Equation 1.

Equation 2 is similar to Equation 1; however, the effects of thermal strain are removed by subtracting out the thermal expansion of the concrete. Figure 12 provides a direct comparison between the contributions of temperature; moisture-related changes, creep and restraint conditions; and moisture- and temperature-related changes, creep and restraint to strain development. The strains in Figure 12 are the average of strains measured from three different slabs.

Temperature was shown to have the greatest effect on strain throughout the year. From the time of construction, the temperature-induced strain follows the seasonal ambient temperature trend, and the magnitude of strain steadily increases until reaching a maximum in the winter. The strain decreases as the ambient temperatures increase in the spring and summer. Moisture-related shrinkage is typically less than thermal strain. From Figure 12, thermal strain was found to be twice as high as moisture-related shrinkage during the first winter after construction. Moisture-related shrinkage is influenced by relative humidity, but unlike temperature, relative humidity does not experience pronounced diurnal fluctuations.

Analysis of Drying Shrinkage and Creep

Figures 13 and 14 show moisture-related shrinkage for various locations at the top and bottom of unrestrained and restrained slabs, respectively. Figure 13 shows strain in the unrestrained slabs, and Figure 14 shows strain in the restrained slabs.

By a comparison of Figure 13*a* and *b*, it can be observed that overall strain in the top sensors is greater than that at the bottom. The effect of moisture-related shrinkage is greatest at the top because it receives greater exposure to the open air and is hence more susceptible to evaporation.

Variations in moisture-related shrinkage occur not only through the depth of the slab but also across the surface of the slab. Moisture-related shrinkage is the lowest at midpanel, where its exposure to the air is limited to the surface of the slab. Moisture-related shrinkage was the highest along the lane–shoulder joint because the tied curb and gutter were not constructed until a few weeks after the lane was paved. Thus, the face of the slab was exposed to the wind and ambient conditions and a larger amount of moisture-related shrinkage occurred. Less moisture-related shrinkage occurred along the transverse joint early on compared with the lane–shoulder joint because its exposure to wind and the ambient climatic conditions was less. The tied centerline joint had even less exposure to wind than the transverse joint, and therefore the moisture-related shrinkage was less than that found at the transverse joint but higher than that at midpanel.

Similar trends were found for the restrained slabs (Figure 14) as were found for the unrestrained slabs. In general, the moisture-related shrinkage increases drastically the first 50 days after construction. The increase in moisture-related shrinkage continues through the winter months but then begins to decrease during the spring when precipitation events occur more frequently. This gradual lessening of moisture-related shrinkage (reversible drying shrinkage) can be seen in Figures 13 and 14 in the range of 150 to 250 days after construction. This phenomenon makes it possible to determine the magnitude of reversible shrinkage that will occur throughout the slab. For the restrained slab compared with the unrestrained slab, the moisture-related shrinkage along the centerline was closer to the moisture-related shrinkage at midpanel because the tie bars keep the centerline joint tight and reduce the exposure to the ambient air and wind.

CONCLUSIONS

An in-depth analysis was provided of the strain that develops as a result of thermal and moisture changes in the slab at both early age (first 72 h after paving) and for the first year after construction. During the first 72 h after paving, the largest strain measured was along the transverse joint. This finding is because of the absence of

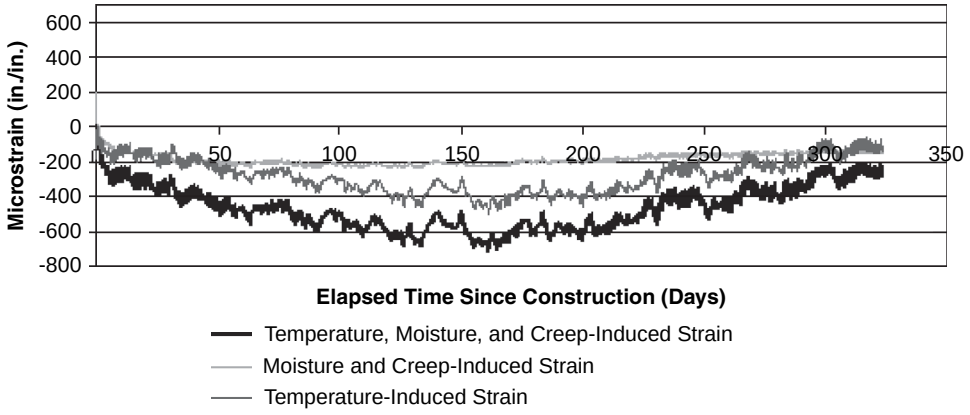

FIGURE 12 Contribution of temperature, creep, and drying shrinkage to total strain at top of unrestrained longitudinal slab.

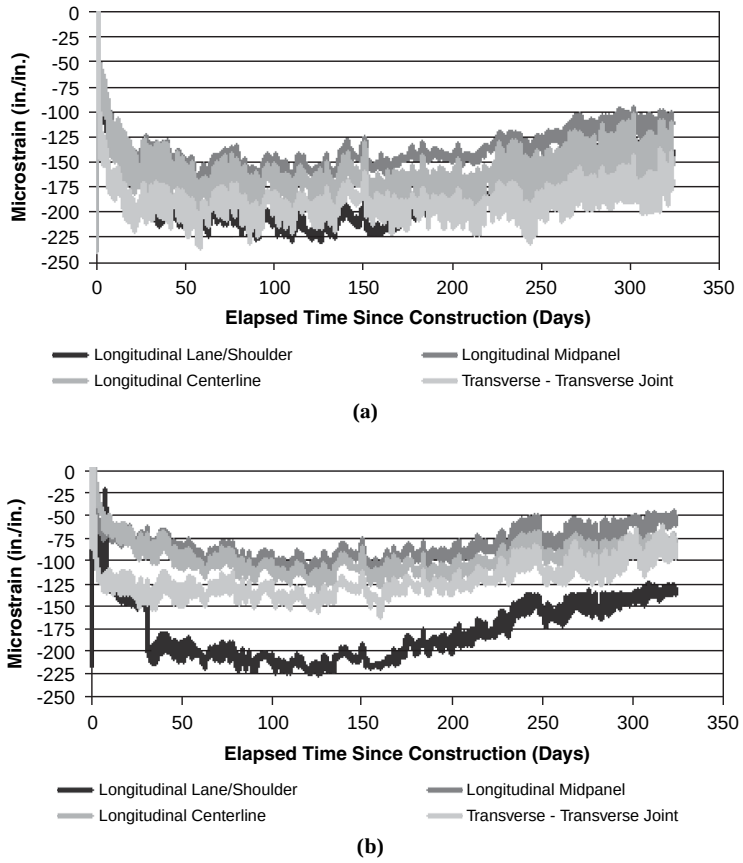

FIGURE 13 Drying shrinkage and creep at locations throughout unrestrained slab.

a curb and gutter, so that there is no restriction on movement from the outside portion of the slab. The longitudinal strain along the centerline exhibits the lowest strain, since movement is restrained by the presence of the previously constructed adjacent lane. The decrease in strain between that measured at the corner in the traverse direction compared with the longitudinal and diagonal along the centerline joint was about 50 μstrain, which corresponds to a stress of 180 psi. The crack width at the joint did not appear to affect the strains measured during the first 72 h after paving.

The magnitude of the strain decreases with increasing slab depth, which indicates that the bond between the base and the bottom of the slab is sufficient to restrain slab deformation. Also, the temperature fluctuations at the bottom of the slab are less than those at the top of the slab.

Much was also learned about the strain that develops in the slab during the first 10 months after construction. The average strain in the fall was around −450 μstrain and that in the winter was −600 μstrain. The ambient temperatures increased during the spring and summer, which resulted in a decrease in the average strain to −250 μstrain. The daily strain fluctuations are the largest in the spring.

Moisture-related shrinkage is typically less than thermal strain. Thermal strain was found to be twice as high as the moisture-related shrinkage during the first winter after construction. A substantial amount of moisture-related shrinkage occurred within the first 50 days after construction. Variations in moisture-related shrinkage occur not only through the depth of the slab but also across the surface of the slab. Moisture-related shrinkage is the lowest at midpanel, where its exposure to the air is limited to the surface of the slab. Moisture-related shrinkage was the highest along the lane–shoulder joint because the tied curb and gutter were not constructed until a few weeks after the lane was paved. Moisture-related shrinkage continues to increase through the winter months but then begins to decrease during the spring, when precipitation events occur more frequently. This gradual lessening of drying shrinkage (reversible drying shrinkage) was quantified.

This study helped to characterize thermal and moisture-related deformation that occurs in the slab shortly after and for the first year after paving. It is extremely important to have a better understanding of the temperature- and moisture-related deformation that occurs in the slab since the current trend is to move toward a more mechanistic approach to pavement design. Once the strains are accurately captured in the field, these data must then be used to ensure that current stress models accurately portray the slab response measured in the field. Future work will include use of these field measurements to verify the finite element models commonly used for pavement design and analysis.

ACKNOWLEDGMENTS

The authors thank the Pennsylvania Department of Transportation and FHWA for their financial and technical support. In addition, they thank all graduate and undergraduate students who assisted in the completion of this project.

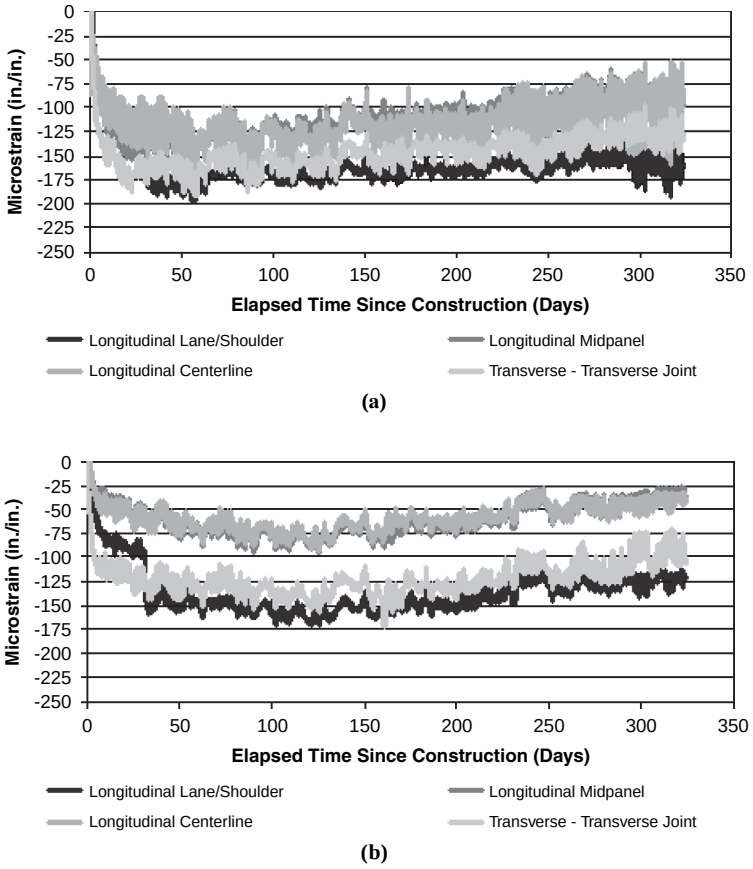

FIGURE 14 Drying shrinkage and creep at locations throughout restrained slab.

REFERENCES

1. Wells, S. A., B. M. Phillips, and J. M. Vandenbossche. *S.R.-22 Smart Pavement Phase I: Early-Age Material Properties and Pavement Response Characteristics for Jointed Plain Concrete Pavements, Phase I Final Report.* Pennsylvania Department of Transportation, June 2005.
2. *Development of 2002 Guide for Design of New and Rehabilitated Pavement Structures, Phase II.* Final Report, NCHRP Project 1-37A. TRB, National Research Council, Washington, D.C., March 2004.
3. Vandenbossche, J. M., and M. B. Snyder. Comparison Between Measured Slab Profiles of Curled Pavements and Profiles Generated Using the Finite Element Method. Presented at 8th International Conference on Concrete Pavements, Denver, Col., Aug. 2005.
4. Hveem, F. N. Slab Warping Affects Pavement Joint Performance. *Journal of the American Concrete Institute,* Vol. 22, No. 10; *Proceedings,* Vol. 47, June 1951.
5. Janssen, D. J. Moisture in Portland Cement Concrete. In *Transportation Research Record 1121,* TRB, National Research Council, Washington, D.C. 1987, pp. 40–44.
6. Poblete, M., R. Salsilli, R. Valenzuela, A. Bull, and P. Spratz. Field Evaluation of Thermal Deformations in Undoweled PCC Pavement Slabs. In *Transportation Research Record 1207,* TRB, National Research Council, Washington, D.C. 1988, pp. 217–228.
7. Reddy, A. S., G. A. Leonards, and M. E. Harr. Warping Stresses and Deflections in Concrete Pavements: Part III. In *Highway Research Record 44,* HRB, National Research Council, Washington, D.C., 1963, pp. 1–24.
8. Wiseman, J. F., M. E. Harr, and G. A. Leonards. Warping Stresses and Deflections in Concrete Pavements: Part II. *Highway Research Board Proceedings,* Vol. 39, 1960, pp. 157–172.

The Rigid Pavement Design Committee sponsored publication of this paper.